Tanzania Journal of Science 49(3): 642-654, 2023
ISSN 0856-1761, e-ISSN 2507-7961


# A Radial Basis Function Neural Network Algorithm for the Simultaneous Retrieval of Two Meteorological Parameters from Solar Radiation

**Nicholas W. Nzala[1,2], Nicolausi Ssebiyonga[2*], Dennis Muyimbwa[2] and Taddeo Ssenyonga[2]**
[1]*Department of Computer Science and Engineering, Makerere University Business School, P. O. Box, 1337, Kampala, Uganda.*
[2]*Department of Physics, Makerere University, P.O. Box 7062, Kampala, Uganda.*
*Email: nicholas.nzala@students.mak.ac.ug, nicolausi.ssebiyonga@mak.ac.ug, dennis.muyimbwa@mak.ac.ug, taddeo.ssenyonga@mak.ac.ug*
**Corresponding author*
Received 13 Jul 2023, Revised 1 Sep 2023, Accepted 7 Sep 2023 Published Sep 2023
**DOI:** https://dx.doi.org/10.4314/tjs.v49i3.8

**Abstract**

Local meteorological parameters are key in understanding the frequency of occurrence of extreme weather conditions such as floods, and droughts, among others. In this study, we present a method for simultaneous retrieval of two weather parameters. The method is based on already measured monthly average values of weather parameters from 2011 to 2016, which were used to train a Feed-forward radial basis function neural network (RBFNN) to obtain a fast and accurate method to compute global solar radiation for specified weather parameters pair. In inverse modelling, a multidimensional unconstrained non-linear optimization was employed to retrieve the weather parameters pair. The new approach was validated using weather parameter data measured at the Department of Physics, Makerere University (0.31° N, 32.58° E, 1200 m). Statistical tools were used to evaluate the method's performance. In the Feed-forward artificial neural network (ANN), the correlation coefficient (R), mean bias error (MnB), root mean square error (RMSE), and mean percentage error (MAPE) were in the ranges 0.80–0.95, -0.0011–0.0077, 0.55–1.04 and 2.49%–5.82%, respectively. The pairs (sunshine hours, relative humidity) and (sunshine hours, minimum temperature) had the highest correlation coefficient of 0.95. In the inverse artificial neural network (ANNi), the R, MnB, RMSE and MAPE were in the ranges 0.3–0.9, 0.01–0.08, 0.51–11.14 and 2.1%–14.5%, respectively. The pair (sunshine hours, relative humidity) had the highest correlation coefficients of 0.92 and 0.62, respectively. The method helps in obtaining weather parameter data sets in places where measuring equipment is lacking or during days when measuring equipment malfunctions.

**Keywords:** Radial basis function, solar radiation, Feed-forward artificial neural network, Inverse artificial neural network, Prediction.

## Introduction

Meteorological parameters such as solar radiation, humidity, sunshine duration, temperature, rainfall, vapour pressure, and wind speed have been used in a wide range of applications such as weather forecasting (Maqsood et al. 2004, Clarke et al. 2022), energy production (Coskun et al. 2011), transportation and aviation (Stocker et al. 2022), agriculture (Ahmad et al. 2017), to mention but a few. Among the meteorological parameters, solar radiation is the most influential (Wald and Wald 2018). It affects all forms of life on Earth such as photosynthesis, water evaporation into the atmosphere, humidity on the ground and in

the atmosphere (Kandirmaz et al. 2014, Wald 2015, Wald and Wald 2018). It is the main driver of plant growth and crop yields (Ceglar et al. 2016, Yang et al. 2020). Solar energy is a renewable energy resource too, and its utilization reduces over-reliance on fossil fuels, hence helping in the mitigation of global warming through the reduction of emission of greenhouse gases to the atmosphere (Fawzy et al. 2020).

Solar radiation is an essential input parameter required when designing and sizing solar energy conversion systems such as photovoltaic, thermal, and thermosyphon applications (Coskun et al. 2011, Sahu et al. 2021). To set up a solar power plant in any location requires realistic measurements of solar radiation and its variation over time with other meteorological parameters. Studies by Mekhilef et al. (2012) and Tasie et al. (2022) showed that different weather parameters greatly influence the amount of solar radiation incident on the Earth's surface. Besides energy systems, knowledge of meteorological parameters is vital in prediction of extreme weather phenomena such as forest fires (Koutsias et al. 2013), hurricanes (Grankov et al. 2021), heat waves (Fischer et al. 2004, Koutsias et al. 2013), floods (Razavi Termeh et al. 2018), droughts (Skierlo et al. 2018), El Nino rains (Wang et al. 2019), and storms (Sarkar et al. 2019). Those extreme weather phenomena have led to the loss of property and life in many different parts of the world (Fischer et al. 2004).

Accurate weather predictions foster tourism and recreational sectors (Parasyris et al. 2022) and are important in the public health sector for the prediction and mitigation of diseases (Agier et al. 2017, Thomson and Mason 2019), cholera (Pascual et al. 2008, Bwire et al. 2013, Simple et al. 2018). There are several prediction techniques employed in estimating meteorological parameters. These include statistical models (Zeroual et al. 1995), analytic models (Njau 1991, Dagestad 2005), empirical methods (Angstrom 1924), and artificial neural networks (ANN) (Mohandes et al. 1998, Nzala et al. 2022). Among the meteorological prediction techniques, the ANN models have proved to be superior because of their capability of automatically resolving relationships between variables without the need for prior assumptions about the nature of their relationships (Gamito et al. 2003) and cater to temporal variations, which is not the case for the classical statistics used in stochastic, analytic, and empirical methods. The high interconnectivity in ANN makes them quite tolerant to errors or noise, in the input data.

The ANNs have been found to perform better than empirical methods in predicting meteorological parameters (Maqsood et al. 2004, Mubiru and Banda 2008). This is because neural network (NN) caters to the nonlinear, non-stationary nature of solar radiation (Sanz and Marqu 2004). The NN learns instead of analysing the complex relationships between the measured data and its effect on the approximation of the parameter (El-Feghi et al. 2013) and is a promising tool to be used in temperature and rainfall prediction since it can handle complex and nonlinear physical variables of the atmosphere ( El-Feghi et al. 2013, Chai et al. 2019, Johnstone and Sulungu 2021).

Most studies have focused on the prediction of solar radiation using meteorological parameters with ANN. Mubiru and Banda (2008) used sunshine hours, maximum temperature, cloud cover, latitude, longitude and altitude to predict solar radiation. Karoro et al. (2011) used sunshine duration to predict solar radiation. Siva Krishna Rao et al. (2018) obtained a relative root mean square error of 3.96% using ANN and a combination of two inputs (difference between minimum and maximum temperature and extraterrestrial radiation) to predict solar radiation and also observed that ANN trained with sunshine hours had a high prediction accuracy. Kumari and Toshniwal (2021) used a combination of two inputs; the difference between maximum and minimum temperatures and sunshine hours to the ANN model and obtained a correlation coefficient of 0.97. According to Moghaddam et al. (2016), the accuracy of the neural network model is influenced by the number of neurons in the hidden layer. Chai et al. (2019) studied

the performance of the RBF model using three different numbers of hidden neurons and the correlation coefficients varied as the number of neurons changed but they observed that the RBF network model produced consistent results throughout the testing using a specific hidden neuron number when the RBF network was retrained and tested.

Gaballa and Cho (2019) obtained RMSE, NMBE and R-squared values of 0.1906, 0.0543, and 0.89, respectively, when they predicted solar radiation using temperature and relative humidity with an artificial neural network. Thallapalli and Prasanna (2022) compared two empirical and one ANN models for solar radiation prediction. They found that the data-driven method provided better predictions than the empirical methods. In this work, we solve an inverse problem where solar radiation is used to predict two meteorological parameters.

The inverse algorithm has been employed in several studies to retrieve different parameters. Stamnes et al. (2013) developed an inversion scheme called Ocean Color: Simultaneous Marine and Aerosol Retrieval Tool (OCSMART). Their OC-SMART retrieval algorithm employs a radial basis function neural network (RBFNN) to establish an analytical relationship between input/retrieval parameters and simulated top-of-atmosphere radiances.

Li et al. (2008) developed a method for optimal estimation to solve the inverse problem by simultaneously retrieving two aerosol parameters that included the AOD at 865 nm, a bimodal fraction of large vs. small particles and three marine parameters that included the chlorophyll concentration, the detrital/dissolved-matter absorption at 443 nm, and the backscattering coefficient at 443 nm from measurements of radiances at eight SeaWiFS channels. The analytic Jacobians were simulated using a coupled atmosphere-ocean radiative transfer model.

Tanaka (2014) used an algorithm that inverts the radiative transfer procedure to retrieve chlorophyll concentrations, suspended organic matter, and yellow substance for the ocean using normalized water-leaving radiance data of the ocean colour and temperature sensor of the Advanced Earth Observing Satellite (ADEOS). This algorithm employed the Stuttgart Neural Network Simulator to construct and train the neural network.

Khatri et al. (2019) developed an algorithm to retrieve cloud optical depth and cloud particle effective radius from spectral zenith radiances observed by narrow field-of-view (FOV) ground-based sky radiometers. An error evaluation study conducted by assuming errors in observed transmittances and ancillary data for water vapour concentration and surface albedo suggests that the errors in input data affect retrieved cloud particle effective radius (CER) more than cloud optical depth (COD). Except for some narrow domains that fall within a COD of < 15, the retrieval errors are small for both COD and CER. The retrieved cloud properties reproduced the broadband radiances observed by a narrow FOV radiometer more precisely than broadband irradiances observed by a wide-FOV pyranometer, justifying the quality of the retrieved product. The retrieved CODs from the sky radiometer and satellite observations showed good agreement.

Ssenyonga et al. (2022) developed an algorithm that simultaneously retrieved five parameters, i.e., two aerosol parameters (aerosol fine-mode fraction and aerosol volume fraction) and three marine parameters (CDOM absorption, chlorophyll concentration and mineral concentration). An algorithm that retrieves sunshine hour values based on solar irradiation was developed by Nzala et al. (2022). They applied optimal estimation by a non-linear function to a cost function of modelled and measured values. The algorithm retrieved sunshine hour values with a correlation coefficient, mean bias and relative root mean square error between the measured and modelled values of 0.924, 0.043 and 0.394, respectively.

To be able to better prepare and reduce the negative effects arising from weather extremes, control diseases, plant growth analyses and all applications where meteorological parameters are needed, there

is a need to have present and future values of meteorological variables. The meteorological data can be obtained through in-situ measurements or by use of retrieval algorithms. In-situ measurements of meteorological parameters are conducted in a few places, and for a limited time in developing countries like Uganda due to the high costs involved in buying and maintaining in-situ measuring equipment. The retrieval inverse ANNi algorithm developed can be used to generate other meteorological parameters datasets in locations where you only have a pyranometer, and to fill gaps in datasets where the measuring instrument malfunctions or is out of calibration. This article aims to address the ease of obtaining meteorological parameters. This study contributes to the understanding, development, and implementation of an ANN model that can be used to retrieve meteorological parameters using radial basis function neural networks.

## Materials and Methods

The meteorological data used in this study was measured over six years. The meteorological parameters include; solar radiation, sunshine hours (SH), relative humidity (RH), minimum temperature ($T_{min}$), maximum temperature ($T_{max}$) and rainfall (RF). Solar radiation and sunshine hours were measured at the Department of Physics, Makerere University, Kampala. Relative humidity, rainfall, minimum and maximum temperatures were obtained from Entebbe Meteorological Station.

## Instruments

The solar radiation used in the study was measured using a pyranometer, sunshine hours were measured using a sunshine duration sensor and relative humidity values were determined using a psychrometer. Minimum and maximum temperatures were measured by the sixth thermometer placed in Stevenson's screen and rainfall was measured using the pluviometer. All of the instruments were ground-based.

The CMP6 pyranometer used to measure global horizontal solar radiation had a spectral range of 285 to 2800 nm, a sensitivity in the range of 5 to 20 $\mu VW^{-1}m^{-2}$ with a field of view of solid angle $2\pi$ steradians. The CSD3 sunshine duration sensor had an operating temperature range of -30–70 °C with an accuracy of 0.1 V.

Relative humidity was determined using the stationary psychrometer placed in a Stevenson's screen. It consists of a pair of dry bulb and wet bulb thermometers of similar size and form securely mounted vertically onto a rectangular wooden frame. A cloth kept wet by water, is wrapped around the bulb of the wet bulb thermometer while the bulb of the dry bulb thermometer is exposed to the atmospheric air. The relative humidity was obtained from the readings of the two thermometers at an instant of time using a psychrometric slide rule (Luther et al. 2005, Ahmad et al. 2017). The sixth thermometer, also kept in the Stevenson's Screen, was used to measure minimum and maximum temperature values.

## Radial basis function neural network (RBFNN) structure

### *Artificial neural networks*

The ANN is an interconnected structure that mimics the human brain and nervous systems primarily made up of processing units called neurons. The neurons are arranged in such a way that the network structure adapts itself to the problem under consideration. ANNs resemble the human brain, they are intelligent with the ability to learn and acquire knowledge, memorize, and create relationships. The strength of the connections between neurons, the architecture pattern followed during construction of the network and the parameters adopted during training of the network determine the processing capability. There are several types of ANN structures which include Multi-Layer Perceptron, Radial Basis Function (RBF) and Support Vector Machine.

***Training and evaluation of the RBFNN***

In this research, the data was divided into two parts; 90% of the data was used in training and 10% was used in the evaluation of the ANN performance. The training of ANN was done using RBF as the activation function. The k-means clustering algorithm was used to determine the centres $C_i$ and the width $\beta$ of the RBF clusters. The weights, $w_{ij}$ were determined using the least mean squares (LMS) algorithm (Broomhead and Lowe 1988, El-Feghi et al. 2013). The RBFNN architecture has three strata namely: an input layer, two hidden layers, and an output layer that are interconnected. The schematic of the RBFNN structure is shown in Figure 1.

In the input layer, raw measured data which is an n-dimensional vector is entered and the data is fed to the hidden layer. In the hidden layer, the data is transformed into a higher dimensional space to make it linearly separable. The hidden layer contains the radial basis function as an activation function. The steps taken in the prediction of parameters in the Feed-forward direction NN and in the inverse ANNi are shown in Figure 2.

The two meteorological parameters ($X_i$) were fed in the input layer, and then the training of the ANN was done using RBF and 90% of the data. The number of neurons in the hidden layer was varied from 2 to 65. From the training, the NN learnt the relationship between solar radiation and any two meteorological parameters.

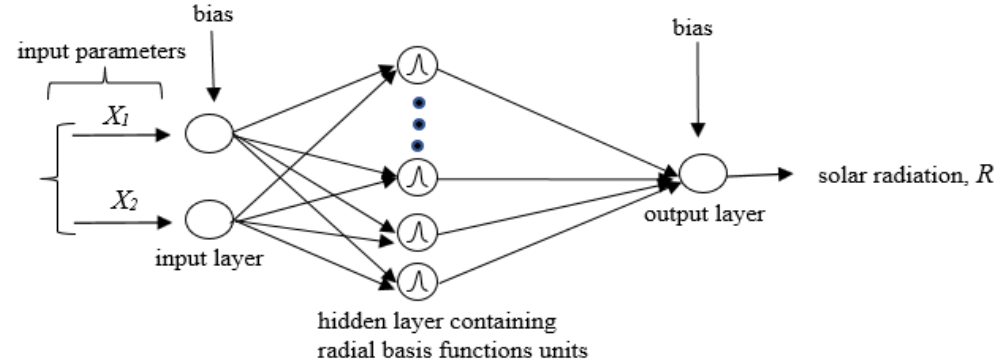


**Figure 1**: Schematic diagram showing RBFNN structure with 3 layers; input layer, hidden layer and the output layer.

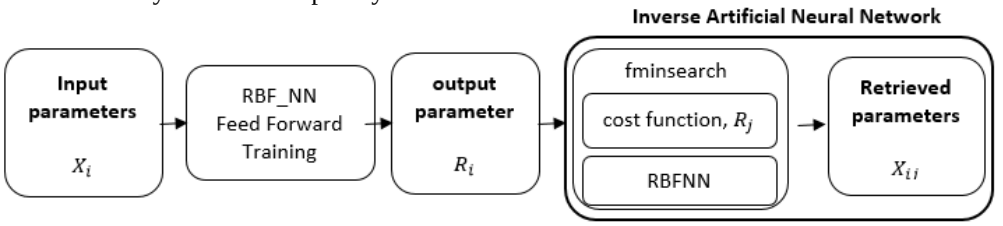


**Figure 2**: Two meteorological parameter retrieval procedure.

According to Satapathy et al. (2021), several radial functions can be used as activation functions in the hidden layer which include: the Gaussian function, multi-quadratic function and inverse multi-quadratic function. The Gaussian RBF function given by Equation (1) (Karlik and Olgac 2011, Fan et al. 2014) is more stable compared to other RBF functions.

$$\phi = e^{-\frac{\|X_i - C_i\|}{2e_i^2}}, \quad (1)$$

where $X_i$'s are input vectors, $C_i$ is the mean of the distribution or $i^{th}$ centrality and is taken as the prototype vector in RBFNN, and $\sigma$ is the $i^{th}$ centrality distance. For the RBFNN, Equation (1) is modified to give Equation (2).

$$\phi = e^{-\beta \| X_i - C_i \|^2}, \quad (2)$$

where $\beta$ controls the width of the Gaussian function curve and $C_i$ is the prototype vector. In the hidden layer where the learning process of the NN occurs, the RBF network positions one or more neurons in the space described by predictor variables. Each neuron has an RBF centred on a point with as many dimensions as the predictor values. Each neuron stores a prototype vector chosen by the system from input data which acts as neuron centres during the training of the ANN. The distance is computed from the point being evaluated to the centre of each neuron or from the prototype vector. The RBF's basic parameters are the centre and width, and their response decreases or increases monotonically with distance from a central point. The RBF and the distance give the weight of each point being evaluated as given in Equation (3).

$$w = \mathrm{RBF}(\mathrm{distance}) \quad (3)$$

In the hidden layer, each input is multiplied with a corresponding weight ($w$), hidden layer bias ($a$) and then a neural network bias ($b$) is added. The output is given in Equation (4).

$$y = a \sum w_i \phi_i + \mathrm{b} \quad (4)$$

For $n$ neurons in the hidden layer, the final output of the RBFNN in the Feed-forward direction is given by Equation (5) according to Fan et al. (2014) and Ssenyonga et al. (2022). This output is a combination of Equation (3) and Equation (4).

$$R_i = \sum_{j=1}^{n} w_{ij} \exp\left[ -a^2 \sum_{k=1}^{N} \left( C_{jk} - X_k \right)^2 \right] + b_i, \quad (5)$$

where $N$ is the total number of input parameters which is equal to two in this study, and the $X_k$'s are the two retrieval meteorological parameters. The purpose of training the RBFNN is to determine the optimized coefficients $w_{ij}$, a, $C_{jk}$ and $b_i$. Those coefficients are then used in the two parameters' retrieval part.

In the inverse retrieval RBFNN, to get the output, the algorithm used a multidimensional unconstrained nonlinear minimization function (fminsearch) based on the Nelder-Mead method (Lagarias et al. 1998). In the inverse RBFNN, the weights were adjusted based on the cost function given in Equation (6).

$$F(w, \mathrm{b}) = \frac{1}{2N} \sum_x \| h(x) - R \|^2, \quad (6)$$

Where $w$ denotes the collection of all weights in the network, $b$ all the biases, $N$ is the total number of training inputs, $h(x)$ is the desired output while $R$ is the vector of outputs from the network when $x$ is input, and the sum is over all training inputs.

**Validation of the Feed-forward ANN and inverse retrieval ANNi**

For both the Feed-forward RBFNN and the inverse ANNi algorithms. The correlation coefficient ($r_i$), normalised mean bias error ($MnB$), root mean square error ($RMSE$) and mean absolute percentage error ($MAPE$) were applied to evaluate the quality of the neural network performances and are given in Equations (7) to (10).

$$r_i = \frac{\sum_i \left( y_{ip} - \bar{y}_{ip} \right)\left( y_{im} - \bar{y}_{im} \right)}{\left\{ \sum_i \left( y_{ip} - \bar{y}_{ip} \right)^2 \right\}^{\frac{1}{2}} \left\{ \sum_i \left( y_{im} - \bar{y}_{im} \right)^2 \right\}^{\frac{1}{2}}}, \quad (7)$$

where $y_{ip}$ and $y_{im}$ are the predicted and measured parameters, while $\bar{y}_{ip}$ and $\bar{y}_{im}$ are their corresponding average values, respectively.

$$MnB = \frac{1}{N} \sum_{i=1}^{N} \frac{\left( y_{ip} - y_{im} \right)}{y_{im}}, \quad (8)$$

where $N$ is the number of observations, the other terms have the same meaning as in equation (7).

$$RMSE = \sqrt{\frac{1}{N} \sum_{i=1}^{N} \left( y_{ip} - y_{im} \right)^2}, \quad (9)$$

where the terms carry the same meaning as in Equation (8), and

$$MAPE = \frac{1}{N}\sum_{i=1}^{N}\left\|\left(\frac{y_{ip} - y_{im}}{y_{im}}\right)\right\| x100, \quad (10)$$

where the terms carry the same meaning as in Equation (8).

**Results and Discussion**

**Feed-forward RBFNN modelling**

Two meteorological parameters were used in the Feed-forward ANN to predict solar radiation. The radial basis function (RBF) was used in training and testing the artificial neural network. The performance of the Feed-forward ANN is shown in Table 1. The input parameters used include; relative humidity (RH), sunshine hours (SH), maximum temperature ($T_{max}$), minimum temperature ($T_{min}$), average temperature ($T_{av}$) and rainfall (RF).

From Table 1, it was observed that the correlation coefficients were from 0.8 to 0.95 for the different combinations of meteorological parameters used in prediction of the magnitude of global solar radiation. Root mean square error (RMSE) varied from 0.55 to 1.04. RMSE is the measure of the accuracy of the model in the prediction of global solar radiation and the normal mean bias error varied from -0.0011–0.0077. The mean percentage errors (MAPE) were between 2.49% and 5.82% and it indicated the percentage error by which the model values differed from the actual measured values. It is observed in Table 1 that in all combinations considered in the prediction of solar radiation, the MAPE was less than 6% which implies that the model in this study predicted solar radiation values with high accuracy. According to Ammar and Xydis (2023), a MAPE of less than 10% indicates very good model accuracy.

**Table 1**: Performance analysis of the Feed-forward RBFNN predicted solar radiation based on two meteorological parameters against pyranometer-measured values

| Parameters used to predict solar radiation | Correlation coefficient (R) | Normal mean bias error (MnB) (%) | Root mean square error (RMSE) | Mean percentage error (MAPE) | Hidden layer neuron number |
|---|---|---|---|---|---|
| RH and $T_{max}$ | 0.91 | -0.11 | 0.71 | 3.2 | 39 |
| SH and RH | 0.95 | 0.31 | 0.55 | 2.6 | 37 |
| SH and $T_{min}$ | 0.95 | 0.21 | 0.55 | 2.5 | 59 |
| RH and $T_{av}$ | 0.81 | 0.77 | 1.00 | 4.5 | 33 |
| RH and $T_{min}$ | 0.80 | 0.52 | 1.04 | 5.0 | 31 |

From Table 1, The best combinations of meteorological parameters in the prediction of solar radiation were SH and RH, SH and $T_{min}$. SH and RH had a mean bias error (MnB), RMSE and correlation coefficient of 0.0031, 0.55 and 0.95, respectively. SH and $T_{min}$ had a mean bias error (MnB), RMSE and correlation coefficient of 0.0021, 0.55 and 0.95, respectively.

The MAPE of 2.6% and 2.5% obtained when (SH, RH) and (SH, $T_{min}$), respectively, supported the observation that those two parameter combinations were the best predictors of the magnitude of solar radiation by the model in this study. Another combination of two parameters which was of acceptable accuracy and is a good predictor of solar radiation with RMSE value less than 1 and MAPE value less than 5% was RH and $T_{max}$ (RMSE = 0.71, MAPE = 3.2%). In addition, it was also observed that the use of RH and RF produced the worst prediction of the magnitude of global solar radiation with a mean bias error (MnB), RMSE, MAPE and correlation coefficient of –0.011, 1.05, 5.82% and 0.27, respectively. This indicated that a combination of humidity and rainfall is not a good predictor of the magnitude of global solar radiation. The correlation coefficients were highest greater than 0.94 when sunshine hours (SH) and any other parameters were used in the prediction of solar radiation. This

may be because sunshine hours have a greater influence on the magnitude of global solar irradiation (Udo 2002). It was observed that to be able to obtain a high correlation coefficient with consistent values of solar radiation irrespective of the number of neurons, the minimum number of neurons in the hidden layer should be in the range of 20 to 65. The use of a combination of relative humidity (RH) and rainfall (RF) in the prediction of solar radiation could not provide a high correlation coefficient even when the neurons were increased to 65.

In this study, a combination of RH and Temperature yielded higher RMSE in the range of 0.55−1.04, a smaller normal bias error in the range -0.0011−0.0077 and higher correlation coefficients of 0.8–0.95 than those obtained by Gaballa and Cho (2019).

**Inverse ANNi Modelling**

In this study, an inverse technique based on RBFNN (ANNi) was used in the prediction of two meteorological parameters simultaneously by using solar radiation. The optimisation function fminsearch minimized the cost function of the estimated and measured solar radiation values. This time, the estimated solar radiation by the trained RBFNN used ANNi modelled meteorological parameter values. Minimised values of the cost function, subject to a tolerance of 1e−12 and maximum function evaluations of 1e10, indicate optimum simulated meteorological parameters that correspond to the measured solar radiation values, thus confirming acceptable retrieval of the parameters. The ANNi performance evaluation is given in Table 2. The accuracy of the inverse ANNi in using solar radiation to simultaneously retrieve two parameters is given by values of the correlation coefficient, mean bias error (MnB), root mean square error (RMSE) and mean absolute percentage error (MAPE) as given in Table 2.

Five pairs of parameters were predicted simultaneously using solar radiation and those included; RH and $T_{max}$; Figure 3 a(i) & (ii), SH and RH; Figure 3 b(i) & (ii), SH and $T_{min;}$ Figure 3 c(i) & (ii), RH and $T_{av}$; Figure 3 d(i) & (ii) and, RH and $T_{min}$; Figure 3 e(i) & (ii). The correlation coefficients for the different pairs of meteorological parameters predicted simultaneously using ANNi are given in Figure 3.

**Table 2**: An investigation of the performance of the inverse artificial neural network (ANNi) in the simultaneous retrieval of two meteorological parameters

| Parameters predicted | R | MnB | RMSE | MAPE (%) |
|---|---|---|---|---|
| RH | 0.58 | 0.08 | 8.07 | 10.2 |
| $T_{max}$ | 0.78 | 0.01 | 1.02 | 2.10 |
| SH | 0.92 | 0.05 | 0.51 | 7.10 |
| RH | 0.62 | 0.05 | 11.14 | 14.5 |
| SH | 0.92 | 0.01 | 0.58 | 6.40 |
| $T_{min}$ | 0.31 | 0.06 | 1.60 | 7.11 |
| RH | 0.51 | 0.07 | 8.20 | 11.0 |
| $T_{av}$ | 0.57 | 0.01 | 1.10 | 3.50 |
| RH | 0.51 | 0.02 | 7.90 | 9.70 |
| $T_{min}$ | 0.30 | 0.03 | 1.40 | 6.10 |

When using ANNi, correlation coefficient, normal mean bias, root mean square error and mean absolute percentage error varied in the ranges; 0.3–0.9, 0.01–0.08, 0.51–11.14 and 2.1%–14.5%, respectively. It was observed that the ANNi predicted SH with the highest correlation coefficient of 0.92 irrespective of a parameter simultaneously predicted with it and sunshine hours have been observed to have a greater influence on the magnitude of global solar irradiation (Udo 2002). The ANNi model predicted minimum temperature with the lowest correlation coefficient of 0.3 as observed in Table 2 and Figure 3. The minimum temperature, which is reached

before sunrise, is affected more by cloud cover, atmospheric and surface boundary conditions than global solar radiation (Karl et al. 1993, Martínez et al. 2010).

The ANNi model was more accurate in predicting sunshine hours with R = 0.92, followed by maximum temperature ($T_{max}$) with R = 0.78 as observed in Table 2 and Figure 3. In the case of simultaneous prediction of the parameters, in Table 2 and Figure 3, it was observed that the model performed better in the simultaneous prediction of SH and RH, RH and $T_{max}$ with correlation coefficients of 0.92 and 0.62, 0.58 and 0.78, respectively. The MAPE values for simultaneous prediction of SH and RH, RH and $T_{max}$ were all less than 15%. MAPE values of less than 25% indicated that model performance was of acceptable accuracy.

Minimum temperature ($T_{min}$) had the lowest correlation coefficient of 0.31 and 0.3 when simultaneously predicted with sunshine hours or relative humidity, respectively. The model fairly simultaneously predicted RH and $T_{av}$ with correlation coefficients of 0.51 and 0.57, respectively using solar radiation. The MAPE for simultaneous prediction of RH and $T_{av}$ were 11% and 3.5%, respectively using solar radiation. The correlation coefficient is one of the most important indicators of model performance. Several studies have used correlation coefficients to rank model performance (El Mghouchi et al. 2016, Uckan and Khudhur 2018).

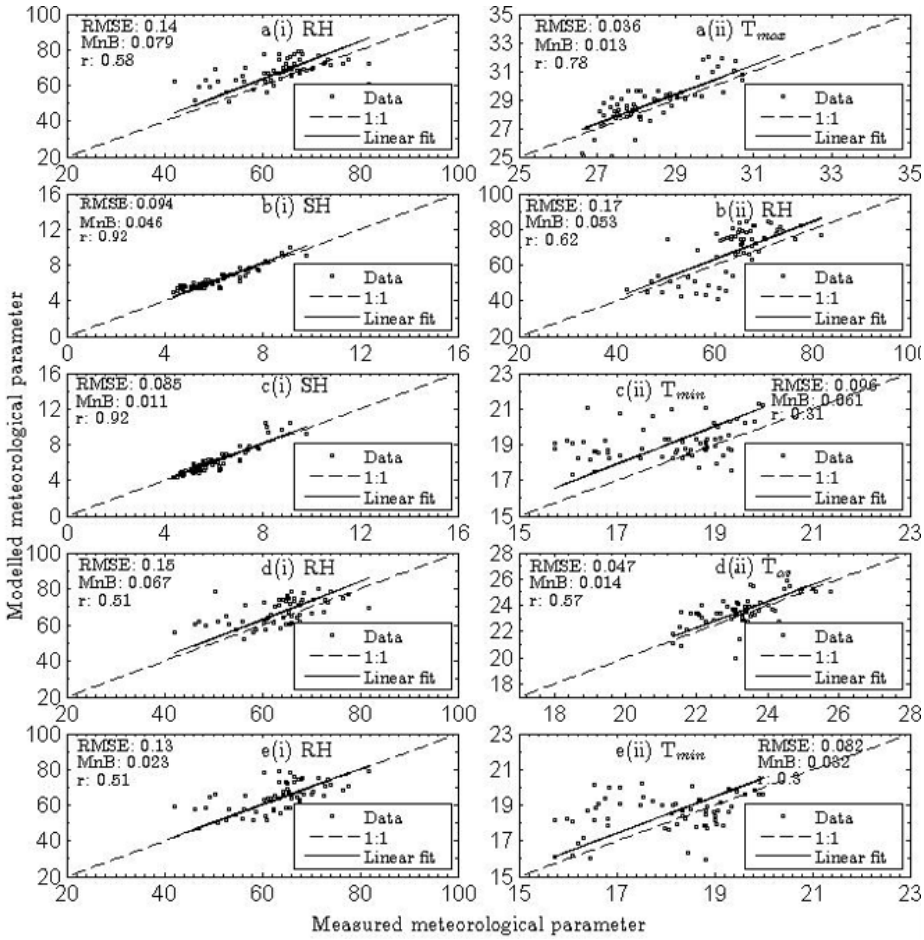


**Figure 3**: Correlation coefficients for the different combinations of two meteorological parameters predicted simultaneously using RBF ANNi based on global solar radiation.

## Conclusions

An inverse artificial neural network algorithm that consists of inverting a radial basis function neural network to retrieve two meteorological parameters simultaneously, based on solar radiation values, has been constructed. Firstly, the RBFNN was appropriately trained so that it could predict solar radiation based on a pair of meteorological parameters with a correlation coefficient of at least 0.8 between the predicted and measured solar radiation values, and saved. Then, the retrieval process implemented optimisation by the fminsearch function of a cost function of measured and inverted RBFNN modelled solar radiation values using ANNi simulated parameters. The inverse ANNi algorithm was tested using data collected at Makerere University Department of Physics for six years and from Entebbe Meteorological Station. The ANNi performed best for simultaneous retrieval of sunshine hours (SH) and relative humidity (RH) with correlation coefficient, RMSE, MnB and MAPE of 0.92, 0.51, 0.05 and 7.10%, respectively, for SH and 0.62, 11.14, 0.05 and 14.54%, respectively, for RH. However, the ANNi algorithm also simultaneously retrieves RH and maximum temperature ($T_{max}$) well with correlation coefficients of 0.58 for RH and 0.78 for $T_{max}$. The ANNi algorithm presents an alternative method for the simultaneous prediction of values of two pairs of meteorological parameters required for monitoring climate change and extreme weather conditions. We recommend that ANNi algorithms for the simultaneous retrieval of three, four and five meteorological parameters be developed. We also propose that ANNi algorithms for the prediction of meteorological parameters in the future, based on moving averages, be developed.

## References


Agier L, Martiny N, Thiongane O, Mueller JE, Paireau J, Watkins ER, Irving TJ, Koutangni T and Broutin H 2017 Towards understanding the epidemiology of Neisseria meningitidis in the African meningitis belt: a multi-disciplinary overview. *Int. J. Infect. Dis.* 54: 103–112.

Ahmad L, Habib R, Sabah K, Syed P and Mahdi S 2017 *Experimental agrometeorology: A practical manual*.

Ammar E and Xydis G 2023 Wind speed forecasting using deep learning and preprocessing techniques. *Int. J. Green Energy 00*(00): 1–29.

Angstrom A 1924 Solar and terrestrial radiation. In *Meterological Society* (Vol. 80, Issue 1).

Broomhead DS and Lowe D 1988 Radial basis functions, multi-variable functional interpolation and adaptive networks: Memorandum no. 4148 royal signals & radar establishment. *Report* 4148.

Bwire G, Malimbo M, Maskery B, Kim YE, Mogasale V and Levin A 2013 The burden of cholera in Uganda. *PLoS Neglect.Trop. Dis.* 7(12).

Ceglar A, Toreti A, Lecerf R, Van der Velde M and Dentener F 2016 Impact of meteorological drivers on regional inter-annual crop yield variability in France. *Agric. Forest Meteorol.* 216: 58–67.

Chai SS, Wong WK, Goh KL, Wang HH and Wang YC 2019 Radial basis function (RBF) neural network: Effect of hidden neuron number, training data size, and input variables on rainfall intensity forecasting. *Int. J. Adv. Sci. Eng. Inf. Technol.* 9(6), 1921–1926.

Clarke B, Otto F, Stuart-Smith R and Harrington L 2022 Extreme weather impacts of climate change: an attribution perspective. *Environ. Res.: Climate* 1(1): 012001.

Coskun C, Oktay Z and Dincer I 2011 Estimation of monthly solar radiation distribution for solar energy system analysis. *Energy* 36(2): 1319–1323.

Dagestad KKF 2005 *Estimating global radiation at ground level from satellite images*. PhD Thesis, *May*. http://web.gfi.uib.no/publikasjoner/pdf/Dagestad.pdf

El-Feghi I, Zubi ZS and Abozgaya A 2013 Air temperature forecasting using radial basis functional artificial neural networks. *Recent Advances in Image, Audio and*

*Signal Processing - Proceedings of the 9th WSEAS International Conference on Remote Sensing (REMOTE '13); Proceedings of the 1st WSEAS International Conference on Image Processing and Pattern Recognition (IPPR '13); Pro*, *December*, 99–104.

El Mghouchi Y, El Bouardi A, Choulli Z and Ajzoul T 2016 Models for obtaining the daily direct, diffuse and global solar radiations. *Ren. Sustain. Energy Rev.* 56: 87–99.

Fan L, Li W, Dahlback A, Stamnes JJ, Stamnes S and Stamnes K 2014 New neural-network-based method to infer total ozone column amounts and cloud effects from multi-channel, moderate bandwidth filter instruments. *Optics Express* 22(16): 19595.

Fawzy S, Osman AI, Doran J and Rooney DW 2020 Strategies for mitigation of climate change: a review. *Environ. Chem. Lett.* 18(6): 2069–2094.

Fischer PH, Brunekreef B and Lebret E 2004 Air pollution related deaths during the 2003 heat wave in the Netherlands. *Atmospheric Environ.* 38(8): 1083–1085.

Gaballa H and Cho S 2019 Prediction of hourly solar radiation using temperature and humidity for real-time building energy simulation. *J. Phys.: Conf. Ser.* 1343(1).

Gamito EJ, David Crawford E and Errejon A 2003 Artificial neural networks for predictive modeling in prostate cancer. *Prostate Cancer: Science and Clinical Practice* 167–172.

Grankov AG, Milshin AA, Novichikhin EP and Shelobanova NK 2021 On the reaction of atmospheric characteristics in the Gulf of Mexico to the origin of hurricanes based on satellite microwave radiometric measurements. *J. Physics: Conf. Ser.* 1991(1).

Johnstone C,and Sulungu ED 2021 Application of neural network in prediction of temperature: a review. *Neural Comput. Appl.* 33(18): 11487–11498.

Kandirmaz HM, Kaba K and Avci M 2014 Estimation of monthly sunshine duration in Turkey using artificial neural networks. *Int. J. Photoenergy* 2014.

Karl T, Jones PD, Knight RW and Plummer N 1993 Trends of daily maximum and minimum temperature. *DigitalCommons @ University of Nebraska- Lincoln Asymmetric*

Karlik B and Olgac AV 2011 Performance analysis of various activation functions in artificial neural networks. *Int. J. Artif. Intellig. Expert Syst.* 1(4): 111–122.

Karoro A, Ssenyonga T and Mubiru J 2011 Predicting global solar radiation using an artificial neural network single-parameter model. *Adv. Artific. Neur. Systems* 2011: 1–7.

Khatri P, Iwabuchi H, Hayasaka T, Irie H, Takamura T, Yamazaki A, Damiani A, Letu H and Kai Q 2019 Retrieval of cloud properties from spectral zenith radiances observed by sky radiometers. *Atmospheric Measurement Techniques* 12(11): 6037–6047.

Koutsias N, Xanthopoulos G, Founda D, Xystrakis F, Nioti F, Pleniou M, Mallinis G and Arianoutsou M 2013 On the relationships between forest fires and weather conditions in Greece from long-term national observations (1894-2010). *Int. J. Wildland Fire* 22(4): 493–507.

Kumari P and Toshniwal D 2021 Advanced machine learning techniques for short-term solar irradiance forecasting. In *First International Conference on AI-ML …* (Vol. 1, Issue 1). Association for Computing Machinery. https://www.aimlsystems.org/2021/docs/doctsymp/65/CameraReady/AI-ML_Pratima.pdf

Lagarias JC, Reeds JA, Wright MH, Wright PE and Optim SJ 1998 *Convergence properties of the Nelder-Mead simplex method in low dimensions** (Vol. 9, Issue 1). http://www.siam.org/journals/ojsa.php

Li W, Stamnes K, Spurr R and Stamnes J 2008 Simultaneous retrieval of aerosol and ocean properties by optimal estimation: SeaWiFS case studies for the Santa Barbara Channel. *Int. J. Remote Sensing* 29(19), 5689–5698.

Luther R, Suter DA and Technology PE 2005

*Psychrometrics*. 213–257.

Maqsood I, Khan MR and Abraham A 2004 An ensemble of neural networks for weather forecasting. *Neural Comput. Appl.* 13(2): 112–122.

Martínez MD, Serra C, Burgueño A and Lana X 2010 Time trends of daily maximum and minimum temperatures in Catalonia (ne Spain) for the period 1975-2004. *Int. J. Climatol.* 30(2): 267–290.

Mekhilef S, Saidur R and Kamalisarvestani M 2012 Effect of dust, humidity and air velocity on efficiency of photovoltaic cells. *Ren. Sustain. Energy Rev.* 16(5): 2920–2925.

Moghaddam AH, Moghaddam MH and Esfandyari M 2016 Stock market index prediction using artificial neural network. *J. Econ. Finance Admin. Sci.* 21(41): 89–93.

Mohandes M, Rehman S and Halawani TO 1998 Estimation of global solar radiation using artificial neural networks. *Renew. Energy* 14(1–4): 179–184.

Mubiru J and Banda EJKB 2008 Estimation of monthly average daily global solar irradiation using artificial neural networks. *Solar Energy* 82(2): 181–187.

Njau EC 1991 Prediction of meteorological parameters-I.-Analytical method. *Il Nuovo Cimento C* 14(5): 473–488.

Nzala, N, Muyimbwa D, Ssebiyonga N and Ssebiyonga T 2022 An inverse artificial neural network algorithm for retrieval of sunshine hours from ground-based global solar irradiation measurements. *E. Afr. J. Sci. Technol. Innov.* 3(4): 1–14.

Parasyris A, Alexandrakis G, Kozyrakis GV, Spanoudaki K and Kampanis NA 2022 Predicting Meteorological Variables on Local Level with SARIMA, LSTM and Hybrid Techniques. *Atmosphere* 13(6).

Pascual M, Cazelles B, Bouma MJ, Chaves LF and Koelle K 2008 Shifting patterns: Malaria dynamics and rainfall variability in an African highland. *Proc. R. Soc. B: Biol. Sci.* 275(1631): 123–132.

Razavi Termeh SV, Kornejady A, Pourghasemi HR and Keesstra S 2018 Flood susceptibility mapping using novel ensembles of adaptive neuro fuzzy inference system and metaheuristic algorithms. *Sci. Total Environ*. 615: 438–451.

Sahu AK, Brahma GS, Aravind R and Swain T 2021 Thermal application of composites of iron and magnesium in thermosyphon solar water heating system. *Heat Transfer* 50(8): 8617–8639.

Sanz BMM and Marqu NJM 2004 Total ozone time series analysis : a neural network model approach. *Nonlin. Proc Geophys.* 11: 683–689.

Sarkar S, Chauhan A and Kumar R 2019 Impact of deadly dust storms (May 2018) on air quality, meteorological, and atmospheric parameters over the Northern parts of India. *GeoHealth* 3(3): 67–80.

Satapathy SK, Mishra S, Mallick PK and Chae GS 2021 ADASYN and ABC-optimized RBF convergence network for classification of electroencephalograph signal. *Personal and Ubiquitous Computing*. https://doi.org/10.1007/s00779-021-01533-4

Simple O, Mindra A, Obai G, Ovuga E and Odongo-Aginya EI.2018 Influence of climatic factors on malaria epidemic in Gulu district, northern Uganda: A 10-year retrospective study. *Malar. Res. Treat.* 2018. https://doi.org/10.1155/2018/5482136

Siva Krishna Rao KDV, Premalatha M and Naveen C 2018 Method and strategy for predicting daily global solar radiation using one and two input variables for Indian stations. *J. Renew. Sustain. Energy* 10(1): 013701.

Skierlo F, Gómez-Hernández JJ and Miegel K 2018 Seasonality of meteorological drought parameters in Germany and their trends due to climate change. *Air Water Components of the Environment* 205–210.

Ssenyonga T, Frette Ø, Hamre B, Stamnes K, Muyimbwa D, Ssebiyonga N and Stamnes JJ 2022 A new algorithm for simultaneous retrieval of aerosols and marine parameters. *Algorithms* 15(1).

Stamnes K, Li W, Fan Y, Hamre, B, Frette O, Folkestad A, Sorensen K and Stamnes JJ 2013 A new algorithm for simultaneous

retrieval of aerosol and marine parameters in coastal environments. *AIP Conference Proceedings* 1531: 919–922.

Stocker J, Johnson K, Forsyth E, Smith S, Gray S, Carruthers D and Chan PW 2022 Derivation of high-resolution meteorological parameters for use in airport wind shear now-casting applications. *Atmosphere* 13(2): 1–19.

Tanaka A 2014 Development of a neural network algorithm for retrieving concentrations of chlorophyll, suspended matter and yellow substance from radiance data of the ocean color and temperature scanner. *J. Oceanogr*. 60: 519-530.

Tasie NN, Sigalo FB, Omubo-Pepple VB and Israel-Cookey C 2022 Modelling of solar power production in dry and rainy seasons using some selected meteorological parameters. *Energy Power Eng*. 14(07): 274–290.

Thallapalli N and Prasanna SVSNDL 2022 Prediction of solar radiation using data driven models. *J. Phys.: Conf. Ser*. 2332(1).

Thomson MC and Mason SJ 2019 Climate information for public health action. In *Routledge Studies in Environment and Health*. https://doi.org/10.4324/9781315115603-10

Uckan İ and Khudhur KM 2018 Estimation and comparison of various global solar radiation models on a horizontal surface in a hot and dry region. *Int. J. Green Energy* 15(5): 358–370.

Udo SO 2002 Contribution to the relationship between solar radiation and sunshine duration in the tropics: A case study of experimental data at Ilorin, Nigeria. In *Turk. J. Phys.* (Vol. 26).

Wald L 2015 Solar radiation energy fundamentals. *Solar Energy Conversion and Photoenergy Systems*, *1*(January 2007).

Wald L and Wald L 2018 *Basics in Solar Radiation At Earth Surface*. https://hal-mines-paristech.archives-ouvertes.fr/hal-01676634/document

Wang Y, Huang P, Wang L, Wang P, Wei K, Zhang Z and Yan B 2019 An improved ENSO ensemble forecasting strategy based on multiple coupled model initialization parameters. *J. Adv. Model. Earth Syst.* 11(9): 2868–2878.

Yang M, Wang G, Ahmed KF, Adugna B, Eggen M, Atsbeha E, You L, Koo J and Anagnostou E 2020 The role of climate in the trend and variability of Ethiopia's cereal crop yields. *Sci. Total Environ.* 723: 137893.

Zeroual A, Ankrim M and Wilkinson AJ 1995 Stochastic modelling of daily global solar radiation measured in Marrakesh, Morocco. *Ren. Energy* 6(7): 787–793.